



Case ML/10857.321

**IN THE UNITED STATES PATENT AND TRADEMARK OFFICE**

2623  
#3  
BT  
01.04.01

In re Application of :  
GHOLAMABBAS HEMIARI, et al. : Examiner:  
Serial No. 09/900,886 : Art Unit:  
Filed: :

For: SYSTEM AND METHOD FOR THE :  
AUTOMATIC EXTRACTION OF LINEAR :  
FEATURES FROM DIGITAL IMAGERY :

RECEIVED  
DEC 10 2001  
Technology Center 2600

**SUBMISSION OF PRIORITY DOCUMENT**

Honorable Commissioner of Patents  
and Trademarks  
Washington, D.C. 20231

Dear Sir:

Applicants hereby submit the attached certified copy of Canadian Patent Application Serial No. 2,313,803 filed on July 11, 2000 with respect to the priority claim in this application. This submission of the priority document is being made in a timely manner. The right of priority has been and was claimed under 35 U.S.C. § 119, the date this application was filed.

It is believed that no fees are due. However, if this determined in incorrect, the Commissioner is hereby authorized to charge any deficiencies to Deposit Account No. 13-2759 and notify the undersigned in due course.

Date: December 6, 2001

MEREK & VOORHEES  
673 South Washington Street  
Alexandria, Virginia 22314  
Telephone: (703) 684-5633

Respectfully submitted,

David H. Voorhees  
Attorney for Applicant  
Reg. No. 33,325

BEST AVAILABLE COPY

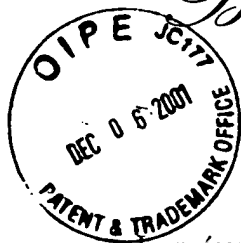


Office de la propriété  
intellectuelle  
du Canada

Un organisme  
d'Industrie Canada

Canadian  
Intellectual Property  
Office

An Agency of  
Industry Canada



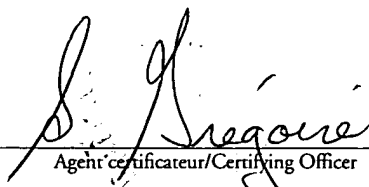
*Bureau canadien  
des brevets  
Certification*

*Canadian Patent  
Office  
Certification*

La présente atteste que les documents  
ci-joints, dont la liste figure ci-dessous,  
sont des copies authentiques des docu-  
ments déposés au Bureau des brevets.

This is to certify that the documents  
attached hereto and identified below are  
true copies of the documents on file in  
the Patent Office.

Specification and Drawings, as originally filed, with Application for Patent Serial No:  
2,313,803, on July 11, 2000, by UNIVERSITE DE SHERBROOKE, assignee of  
Gholamabbas Hemiani, Denis Morin and Dong-Chan He, for "Automatic Extraction of  
Linear Features from Digital Imagery"

  
Agent certificateur/Certifying Officer

November 27, 2001

Date

Canada

(CIPO 68)  
01-12-00

OPIC  CIPO

**ABSTRACT OF THE DISCLOSURE**

A method and apparatus for the automatic extraction of linear features from digital imagery is disclosed herein. The proposed  
5 methodology derives from the Radon transform, yet has none of its basic disadvantages. Indeed, it is not limited solely to extracting straight lines, there are no false peaks or *virtual maxima* (peaks that do not represent the real line on the input image) in the transformed plane and the process does not have difficulty detecting line segments which are significantly  
10 shorter than image dimensions.

---

**TITLE OF THE INVENTION**

Automatic Extraction of Linear Features from Digital Imagery

5

**FIELD OF THE INVENTION**

10                   The present invention relates to digital imagery. More specifically, the present invention is concerned with the automatic extraction of linear features from digital imagery.

**BACKGROUND OF THE INVENTION**

15

                  With the recent, rapid development of computer tools, digital image processing has become an efficient, economic, and convenient means for obtaining qualitative and quantitative information in different fields such as remote sensing, cartography, robotics, and materials. Indeed, digital image processing makes it possible to qualitatively describe images from various sources in terms of pattern recognition to identify and isolate contained objects. One of the major subclasses of contained objects often present in digital images is the linear features. Automatic detection of linear features from digital images plays an important role in pattern recognition and digital image processing.

20

25

                  A variety of techniques and many algorithms have

---

emerged to automatically extract linear features from digital images. These techniques can be classified into two main categories: local methods (which are, based on local operators such a mobile kernel) and global methods (which focus on mathematical transformations, such as  
5 *Hough* transforms) [1].

Local methods for automatically extracting linear features exploit local variations of pixel intensity in a small neighborhood by calculating of the gradients in small, limited-size windows in the image,  
10 e.g.,  $3 \times 3$  or  $5 \times 5$  [2][3][4][5][6][7][8][9]. A number of researchers have examined mathematical morphology as a means of extracting linear features [10][11][12][13][14]. The problems pertaining to this technique arise from the number of human decisions required to reconnect and rebuild line segments, which increases processing time. Multi-dimensional  
15 line detection is the other technique for detecting for linear features that collects different spectral information for the same scene and may highlight different parts of lines [15]. The first stage of this method for obtaining the combined images requires several transformations of multiple original bands. Human intervention is needed to select the best-  
20 combined image. Another approach to linear-feature extraction involves knowledge-based systems, which need more information than a simple digital image for line extraction [16][17][18].

These local methods generally remain inefficient  
25 because they fail to have a global view of the linear features in a digital image. One problem common to all of these methods is that the resulting extracted line images contain a fair amount of noise, while the detected

---

lines are incomplete and geometrically shifted. These difficulties are magnified by intersections and linear features that display some curvature [19][20][1]. In addition, these methods turn in exceptionally long processing times when extracting features from large images [16].

5

The *Radon* transform and its derivative, the Hough transform, are the most frequently used approaches as global methods for detecting linear features [21][22][23][24]. In principle, a straight line from the input image is transformed into a digital peak (a light or dark pixel, compared to its neighborhood) in the transformed plane. In this case, it is easier to detect a peak in the transformed plane than straight line detection in the input image. There are three basic limitations for these methods that sorely restrict their applications and their utility in practice.

10

Firstly, the Hough transform-based methods are limited solely to extracting straight lines [21]. Therefore, linear features that span the entire image but display some curvature may not produce suitable peaks or troughs in the transform plane. This restriction is linked directly to the basic definition of the method.

15

Secondly, there are false peaks or *virtual maxima* (peaks that do not represent the real line on the input image) in the transformed plane. These false peaks considerably lower the quality of the results by increasing the error of commission. When the line density in the input image is high, eliminating the false peaks from transformed plane seriously limits these methods.

20

25

The last methodological inconvenience of these approaches is the ignorance of the nature of the detected lines. Since intensity integration in the transformation process is performed over the entire length of the image, the process can have difficulty detecting line segments which are significantly shorter than image dimensions [21][25][26]. Neither can it provide information about the positions of the endpoints of these shorter line segments or line length.

## 10 **OBJECTS OF THE INVENTION**

An object of the present invention is therefore to provide an improved approach for the extraction of linear features.

15 Other objects, advantages and features of the present invention will become more apparent upon reading of the following non-restrictive description of preferred embodiments thereof, given by way of example only with reference to the accompanying drawings.

20

## **BRIEF DESCRIPTION OF THE DRAWINGS**

In the appended drawings:

25 Figures 1a, 1b and 1c are a flowchart and a legend of the proposed technology;

---

Figure 2 is a binary image simulated to showcase the method's ability to extract all lines without consideration for the slope line; extract the lines having a shorter length of the image dimension; and locate extracted lines accurately;

5

Figure 3 is a binary image 2 obtained by applying the implemented algorithm to the binary image of Figure 2;

Figure 4 is a binary image simulated in order to demonstrate the method's performance in extracting curved as well as straight lines;

10

Figure 5 is a binary image produced by applying the implemented algorithm to the binary image of Figure 4;

15

Figure 6 is a binary image of a part of a digitized road map of the city of Sherbrooke; and

Figure 7 is a binary image 6 produced by applying the implemented algorithm to the binary image of Figure 6.

20

### **DESCRIPTION OF THE PREFERRED EMBODIMENT**

The proposed methodology derives from the Radon transform, yet has none of its basic disadvantages already mentioned hereinabove. It also builds on a solid mathematical base which

25



demonstrates the conceptual feasibility of the new method mathematically. An algorithm has also been developed and implemented in order to achieve a concrete realization of the innovative method in a real context.

5

In following subsections, the mathematical base as well as general procedures for a algorithmic development of our proposed method will be presented in detailed.

## 10 MATHEMATICAL DEVELOPMENT

### Continuous function

Let  $g(x,y)$  be a continuous signal of the continuous variables  $x$  and  $y$  and let  $\xi$  denote a  $\eta$ -dimensional parameter vector defined as:

$$\xi = (\xi_1, \xi_2, \xi_3, \dots, \xi_i, \dots, \xi_\eta) \quad (1)$$

20 where  $\xi$  spans the parameter domain.

For a two-dimensional continuous function, the parameter vector can be defined as:

$$\xi = (\xi_1, \xi_2, \xi_3) \quad \eta = 3 \quad (2)$$

or:

$$\xi = (\alpha, \beta, \gamma) \quad (3)$$

hence:

$$g(x, y) = \phi(x, y; \xi) = y - \alpha x^2 - \beta x - \gamma \quad (4)$$

5                      The Radon transform  $\check{g}(\xi)$  of function  $g(x, y)$  is defined as:

$$\check{g}(\xi) = \int_{-\infty}^{\infty} \int_{-\infty}^{\infty} g(x, y) \delta(\phi(x, y; \xi)) dx dy \quad (5)$$

10    where  $\delta(\cdot)$  denotes the *Dirac delta function*.

Using the definition (5) of Radon transform, curves expressed by the next parameter form can be detected:

$$15 \quad \phi(x, y; \xi) = 0 \quad (6)$$

Substituting the relation (4) into equation (5), we find:

$$\check{g}(\alpha, \beta, \gamma) = \int_{-\infty}^{\infty} \int_{-\infty}^{\infty} g(x, y) \delta(y - \alpha x^2 - \beta x - \gamma) dx dy \quad (7)$$

20    where  $y = \phi(x; \xi)$  represent the transformation curve.

Using proprieties of delta function, equation (7) becomes:

$$\tilde{g}(\alpha, \beta, \gamma) = \int_{-\infty}^{\infty} \int_{-\infty}^{\infty} g(x, y) \delta(y - \alpha x^2 - \beta x - \gamma) dx dy = \int_{-\infty}^{\infty} g(x, \alpha x^2 + \beta x + \gamma) dx \quad (8)$$

At this stage, the transformation curve is defined as a  
 5 polynomial function of second degree using the delta function as below:

$$g(x, y) = \delta(y - \phi(x; \xi^*)) \quad (9)$$

where the parameter vector of this curve is:

$$\xi^* = (\alpha^*, \beta^*, \gamma^*) \quad (10)$$

Using equations (4), (9) and (10), we find:

$$g(x, y) = \delta(y - (\alpha^* x^2 + \beta^* x + \gamma^*)) \quad (11)$$

According to definition of the Radon transform:

$$\begin{aligned} \tilde{g}(\xi) &= \int_{-\infty}^{\infty} \delta(\phi(x; \xi) - \phi(x; \xi^*)) dx \\ &= \int_{-\infty}^{\infty} \sum_{i=1}^I \frac{\delta(x - x_i)}{\left| \frac{\partial \phi(x; \xi)}{\partial x} - \frac{\partial \phi(x; \xi^*)}{\partial x} \right|} dx \\ &= \sum_{i=1}^I \frac{1}{\left| \frac{\partial \phi(x_i; \xi)}{\partial x} - \frac{\partial \phi(x_i; \xi^*)}{\partial x} \right|} \end{aligned} \quad (12)$$

Substitution of parameter vectors (3) and (10) into the transform definition (12) gives:

5

$$\begin{aligned}\tilde{g}(\alpha, \beta, \gamma) &= \int_{-\infty}^{\infty} \delta((\alpha x^2 + \beta x + \gamma) - (\alpha^* x^2 + \beta^* x + \gamma^*)) dx \\ &= \int_{-\infty}^{\infty} \sum_{i=1}^1 \frac{\delta(x - x_i)}{\left| \frac{\partial(\alpha x^2 + \beta x + \gamma)}{\partial x} - \frac{\partial(\alpha^* x^2 + \beta^* x + \gamma^*)}{\partial x} \right|} dx \quad (13)\end{aligned}$$

10

$$= \frac{1}{\left| \frac{\partial(\alpha x^2 + \beta x + \gamma)}{\partial x} - \frac{\partial(\alpha^* x^2 + \beta^* x + \gamma^*)}{\partial x} \right|}$$

Finally, we find:

$$\tilde{g}(\alpha, \beta, \gamma) = \infty \quad \text{pour} \quad \alpha = \alpha^* \quad \text{et} \quad \beta = \beta^* \quad \text{et} \quad \gamma = \gamma^*$$

$$0 < \tilde{g}(\alpha, \beta, \gamma) < \infty \quad \text{pour} \quad \text{autres cas}$$

15 (14)

Equation (14) shows that the Radon transform of a polynomial function of second degree will give an infinite value (a peak) in the parameter domain, when parameters of this function are precisely determined. In addition, this equation confirm that the parameter domain

20

will contain some other non-zero values because of parameters values which have some similarity with real parameter values of the polynomial function in question.

5 In the light of the mathematical demonstration presented above, three important issues are concluded:

- i) The Radon transform of a two-dimensional plane containing a polynomial function of second degree is a Euclidean tree-dimensional space;
- 10 ii) this polynomial function is mapped into a unique point in the tree-dimensional space;
- iii) position of this point in the tree-dimensional space determines the polynomial function parameters.

15 The following subsection provides a discrete approximation to the Radon transform for a polynomial function of second degree. This discrete approximation is the key of the algorithmic development of the polynomial function in question.

## 20 Discrete Function

Discrete Radon transform of a discrete function  $\phi(m;l,k,h)$  is defined as:

$$25 \quad \tilde{g}(l,k,h) = \sum_{m=0}^{M-1} g(m, \phi(m;l,k,h)) = \sum_{m=0}^{M-1} g(m, n(m;l,k,h)) \quad (15)$$

where :

$$\phi(m;l,k,h) = n = \left[ \frac{\phi(x_{\min} + m\Delta x; \theta(l,k,h) - y_{\min})}{\Delta y} \right] \quad (16)$$

and

$$\begin{cases} x_m = x_{\min} + m\Delta x & m = 0, 1, \dots, M \\ y_n = y_{\min} + n\Delta y & n = 0, 1, \dots, N \end{cases} \quad (17)$$

5

where M and N are the discrete plane dimensions and  $\Delta x$ ,  $\Delta y$  are sampling intervals of this plane.

For a polynomial function of second degree expressed

10 as  $y - \varepsilon x^2 - \rho x - \tau = 0$ , the Radon transform is:

$$\tilde{g}(l,k,h) = \Delta x \sum_{m=0}^{M-1} g(x_m, \varepsilon_l x_m^2 + \rho_k x_m + \tau_h) \quad (18)$$

with:

$$\begin{cases} \varepsilon_l = \varepsilon_{\min} + l\Delta\varepsilon & l = 0, 1, \dots, L \\ \rho_k = \rho_{\min} + k\Delta\rho & k = 0, 1, \dots, K \\ \tau_h = \tau_{\min} + h\Delta\tau & h = 0, 1, \dots, H \end{cases} \quad (19)$$

15

where L, K and H represent dimensions of Radon domain and  $\Delta\varepsilon$ ,  $\Delta\rho$  and  $\Delta\tau$  are sampling intervals of this domain.

Using relation (19), the function  $n(m;l,k,h)$  of relation

20 (16) becomes:

12

$$n(m; l, k, h) = \left[ \frac{\varepsilon_l x_m^2 + \rho_k x_m + \tau_h - y_{\min}}{\Delta y} \right] \quad (20)$$

With substituting the relation (17) in the previous equation, we find:

5

$$n(m; l, k, h) = \left[ \frac{\varepsilon_l (x_{\min} + m\Delta x)^2 + \rho_k (x_{\min} + m\Delta x) + \tau_h - y_{\min}}{\Delta y} \right] = n^* \quad (21)$$

For simplifying, the previous equation can be expressed as:

10

$$n^* = \alpha m^2 + \beta m + \gamma \quad (22)$$

where:

$$15 \quad \begin{cases} \alpha = \frac{\varepsilon_l \Delta x^2}{\Delta y} \\ \beta = \frac{(2x_{\min} \varepsilon_l + \rho_k) \Delta x}{\Delta y} \\ \gamma = \frac{\varepsilon_l x_{\min}^2 + \rho_k x_{\min} + \tau_h - y_{\min}}{\Delta y} \end{cases} \quad (23)$$

According to the equation (19), once the Radon domain parameters has been initialized, using equations (21), (22) and (23) this

domain is determined for all of two-dimensional plane points (X,Y).

### **Algorithmic development**

5                   The concrete achievement of the proposed method is schematized in a flowchart presented in Figures 1a and 1b. This flowchart illustrates also all essential instructions for an algorithmic development of the proposed technology.

#### **10    1) Input image**

Represents the digital input image.

#### **2) Design the discrete parameter domain**

The parameter vector of the transformation is defined in this step as  
15   described in equations (1), (2) and (3) in subsection (3.1) (Mathematical Development).

$$\xi = (\xi_1, \xi_2, \xi_3, \dots, \xi_i, \dots, \xi_\eta) \quad (1)$$

$$\xi = (\xi_1, \xi_2, \xi_3) \quad \eta = 3 \quad (2)$$

$$20 \quad \xi = (\alpha, \beta, \gamma) \quad (3)$$

#### **3) Length of lines to be detected**

Input of the interval of line length (i.e. lines between 5 and 220 pixels).

---



**4) Initialize parameter domain**

This step is for initializing the numerical values of discrete parameters

$\varepsilon_{\min}$ ,  $\Delta\varepsilon$ ,  $\rho_{\min}$ ,  $\Delta\rho$ ,  $\tau_{\min}$ ,  $\Delta\tau$ ,  $L$ ,  $K$  et  $H$ , as described in equation (19) and

$x_m, y_n$ ,  $\Delta x$ ,  $\Delta y$ , as described in equation (17) ( $M$  and  $N$  correspond to the

5 dimension of digital input image).

$$\begin{cases} x_m = x_{\min} + m\Delta x & m = 0, 1, \dots, M \\ y_n = y_{\min} + n\Delta y & n = 0, 1, \dots, N \end{cases} \quad (17)$$

10

$$\begin{cases} \varepsilon_l = \varepsilon_{\min} + l\Delta\varepsilon & l = 0, 1, \dots, L \\ \rho_k = \rho_{\min} + k\Delta\rho & k = 0, 1, \dots, K \\ \tau_h = \tau_{\min} + h\Delta\tau & h = 0, 1, \dots, H \end{cases} \quad (19)$$

**5) Start of 1<sup>st</sup> loop (for every position in the parameter domain)**

15 It's a loop for determining every possible combination of  $\varepsilon_l$ ,  $\rho_k$  et  $\tau_h$  as described in equation (19) by incrementing tree values of  $l$ ,  $k$  and  $h$  ( $0 < l < L$ ,  $0 < k < K$ ,  $0 < h < H$ ).

**20 6) Computation of line / curve deterministic parameters**

15

In this step, the deterministic parameters  $\alpha$ ,  $\beta$  and  $\gamma$  are computed by using equation (23).

$$\begin{cases} \alpha = \frac{\varepsilon_l \Delta x^2}{\Delta y} \\ \beta = \frac{(2x_{\min} \varepsilon_l + \rho_k) \Delta x}{\Delta y} \\ \gamma = \frac{\varepsilon_l x_{\min}^2 + \rho_k x_{\min} + \tau_h - y_{\min}}{\Delta y} \end{cases} \quad (23)$$

5

**7) Start of 2<sup>nd</sup> loop (determination of corresponding pixel's co-ordinates)**

In this loop, for each value of  $m$  ( $0 < m < M$ ), a new parameter  $n^*$  is computed by using equation (21).

10

$$n(m; l, k, h) = \left\lceil \frac{\varepsilon_l (x_{\min} + m \Delta x)^2 + \rho_k (x_{\min} + m \Delta x) + \tau_h - y_{\min}}{\Delta y} \right\rceil = n^* \quad (21)$$

**8) Finding the nearest pixel to determined co-ordinates in the input image**

15

In this step, the determined co-ordinates  $(m, n^*)$  of the previous step are used to find the nearest neighbour approximation pixel  $P(m, n)$  within the input image.

20

**9) Numerical value of pixel is zero**

It's a verification step for numerical value of determined pixel  $P(m, n)$  in step 8.

**5 10) Increment number of zero pixels**

If the numerical value of determined pixel  $P(m, n)$  in step 9 is zero, the number of zero pixels will be incremented.

**11) Save the pixel's co-ordinates in the 1<sup>st</sup> layer of database**

10 The pixel's co-ordinates  $m$  and  $n$  are stored in the first layer of the database.

**12) Save the obtained value in the 4<sup>th</sup> layer of database**

15 The numerical value of the determined pixel  $P(m, n)$  in step 9 is stored in the 4<sup>th</sup> layer of database.

**13) Increment number of non zero pixels**

If numerical value of the determined pixel  $P(m, n)$  in step 9 is not zero, the number of non zero pixels will be incremented.

20

**14) Save the obtained value in the 3<sup>rd</sup> layer of database**

The numerical value of the corresponding pixel is stored in the 4<sup>th</sup> layer of the database.

**25 15) Save the pixel co-ordinates in the 2<sup>nd</sup> layer of database**

The non-zero pixel's co-ordinates  $m$  and  $n$  are stored in the second

---

layer of the database.

**16) Accumulation of pixel numerical values**

In this step, the numerical values of pixels are accumulated.

5

**17) Save the obtained value in the 5<sup>th</sup> layer of database**

The value obtained in the step 16 is stored in the 5<sup>th</sup> layer of the database.

**18) End of the 2<sup>nd</sup> loop**

10 This is the end of the 2<sup>nd</sup> loop (loop for all values of  $m$   $0 < m < M$ ).

**19) End of the 1<sup>st</sup> loop:**

This is the end of the 1<sup>st</sup> loop (loop for all values of  $l$ ,  $k$  and  $h$ ).

15 **20) Start of the 3<sup>rd</sup> loop (for every cell in the 3<sup>rd</sup> layer)**

It's a loop for recalling all the numerical values of non-zero pixels already stored in the 3<sup>rd</sup> layer of the database.

**21) The value is inside the predefined range**

20 In this step, the determined numerical value of precedent step is verified to find if it's inside the predefined interval in step 3.

**22) Provided database**

It's the provided database.

25

**23) Finding endpoints of the line**

If the respond of step 21 is positive, stored co-ordinates of the corresponding pixels in the 3<sup>rd</sup> layer of the database are recalled. Then, in the input image, the numerical values of these pixels will be verified to find endpoints of the corresponding line.

5

**24) Restoration of determined line in output image**

In this step, by using the stored deterministic parameters of the line and the line endpoints that are found in the precedent step, the detected line will be restored in the output image.

10

**25) Save all the extracted line information in a new database**

All the information about extracted lines, such as endpoints, lengths, etc. are stored in a new database.

**15 26) End of the 3<sup>rd</sup> loop**

This is the end of the 3<sup>rd</sup> loop (loop for all cells in the 3<sup>rd</sup> layer of the database).

**27) End of algorithm**

20 The end of algorithm.

**FEATURES AND OPERATION OF THE INVENTION**

We have developed a new global method that is capable

25 of:

- detecting and extracting the lines from a digital image with any
-

curvature;

- discarding the virtual maxima on the Hough or on the Radon transformed plane;
- locating every line segment in the input image (endpoints and length).

5

### **Demonstration and Discussion**

For a visual demonstration, the urban road network detection of the city of Sherbrooke from satellite imagery has been selected as an application.

10

The binary image of Figure 2 was simulated to showcase the method's ability to:

- i) extract all lines without consideration for the slope line;
- ii) extract the lines having a shorter length of the image dimension;
- 15 iii) locate extracted lines accurately.

Figure 3 is a binary image obtained by applying the implemented algorithm to the image of Figure 2. The absolute similarity of Figure 3 with Figure 2 demonstrates clearly the accuracy of three abilities  
20 of the method as described above.

The binary image of Figure 4 was simulated in order to demonstrate the method's performance in extracting curved as well as straight lines. The binary image illustrated in Figure 5 was produced by  
25 applying the implemented algorithm to the binary image of Figure 4. The last image demonstrates this performance.

The binary image of Figure 6 is part of a digitized road map of the city of Sherbrooke. Finally, the binary image of Figure 7 was produced by applying the implemented algorithm to the binary image of Figure 6. A comparison of the binary images of Figures 6 and 7 reveals that the restrained roads in the input image have been extracted in detail and with high geometric precision.

#### **ADVANTAGES AND DISADVANTAGES OF THE INVENTION VERSUS COMPETITIVE 10 TECHNOLOGIES**

To the best of our knowledge, there is no operational algorithm that automatically extracts line features and provides accurate, acceptable results either referred to in the literature or available on the market. The interactive and semi-automatic methods remain the most used.

Of the local methods, LINDA (Linear-featured Network Detection and Analysis) system [2][7][27], based on the profile intensity analysis of the pixel line, is the most recent and the most representative method. With all of basic disadvantages of the local methods (cf. the first paragraph of page 5), the LINDA system is far from being operational with respect to systematically and automatically processing a large set of images.

25

As for the global method, the Hough transform is

---

probably the method most frequently mentioned and used by scientific researchers in various fields [9][21][25]. Due to its basic limitations as discussed above, the method is to a large degree limited to a specific type of application in which lines are straight, continuous, and of low density.

5

When compared to techniques reported in the scientific literature or now commercially available, the proposed method is unique, since it can extract curved lines of any length with a high degree of accuracy. Our method identifies every line or line segment, labeling its  
10 length, its curvature, and endpoint coordinates in a database. Moreover, the database can be easily integrated into any geographic or spatial information system. Consequently, everything points to our method as having significant potential. It could lead to the development of robust, operational software to automatically extract line features from any kind of  
15 digital image from various sources.

#### EXAMPLES OF FIELDS OF APPLICATIONS

The method is of broad interest and makes a general  
20 contribution to the field of pattern recognition and digital image processing, regardless of the nature or source of the digital image. It could be used in a vast number of fields and application, of which the following are a sampling.

- 25 A) Remotely sensed imagery
- Extracting and updating road maps.
-



- Planimetric cartography, geology, and hydrology.
- Mapping power-lines, pipelines, and railways.
- Tracking cycle trails, ORV trails, and the like.

5 B) Medical imagery

- Detecting of arteries, blood vessels, tumors, etc;

C) Imagery from other source

- Electrical circuits and the like.

10

References:

- [1] Wang, D., He, D.-C., Wang, L., et Morin, D. (1996) L'extraction du réseau routier urbain à partir d'images SPOT HRV. INT. J. Remote Sensing, vol.17, n°. 4, p. 827-833.

15

- [2] Groch, W.D. (1982) Extraction of Line Shaped Objects from Aerial Images using a Special operator to analyse the Profiles of Functions. Computer Graphics and Image Processing, vol.18, p. 347-358.

- 20 [3] Lacroix, V., et Acheroy, M. (1998) Feature extraction using the constrained gradient. ISPRS Journal of Photogrammetry and Remote Sensing, vol.53, p. 85-94.

- 25 [4] Nevatita, R. et Babu, K. R. (1980) Linear Feature Extraction and Description. Computer Graphics and Image Processing, vol.13, p. 257-269.

- [5] Schanzer, D., Plunkett, G. W. et Wall. Da. (1990) Filters for Residential Road Delineation from SPOT LPA Imagery. GIS FOR 1990s, 801, Conference Proceedings.
- 5 [6] Ton, J. (1989) Automatic Road Identification and labelling in Landsat 4 TM Images. Photogrammetria, vol.43, n°.5, p. 257-276.
- [7] Wang, J.F., Treitz, P. M., et Howarth, P. J. (1992) Road network detection from SPOT imagery for updating geographical information systems in rural-urban fringe. Geographical Information Systems, 10 vol.6, n°2, p. 141-157.
- [8] Wang, J.F., et Howarth, P.J. (1987) Methodology for Automated Road Network Extraction from Landsat TM Data. Proc. Ann ASPRS/ACSM Convention (Baltimore, MD), vol.1, p. 429-438. 15
- [9] Wang, J.F., et Wenhong, L. (1993) Evaluation of Road Detection Methods Using Multi Band remote sensing Images. Canadian Symposium on Remote Sensing, 16th, L'AQT/CRSS. 20
- [10] Destival, I. et Men, H. L. (1986) Detection of Linear Networks on Satellite Images. Photogrammetric Engineering and Remote Sensing, vol.54, n°. 10, p. 1551-1555.
- 25 [11] Ferrand, R., et Marty, H.M. (1985) Computer Processing Test on a Simulated SPOT Image of Toulouse (France). Photo-Interpretation, vol.3, p. 39-45.
-

- [12] O'Brien, D. (1988) Automatic extraction of road networks from digital imagery. Proceeding of the International Symposium on Topographic Applications of SPOT Data, October 13-14, (Sherbrooke, Quebec, Canada; Canadian Institute of Surveying and Mapping), p.273-287.

5

- [13] Peters, R.A. (1995) A New Algorithm for Image Noise Reduction Using Mathematical Morphology. Transactions on image processing, vol.4, n°. 5, p. 554-568.

- 10 [14] Voiron, Ch. (1995) Analyse spatiale et analyse d'image. Montpellier, GIP RECLUS, p.190.

- 15 [15] Chittineni, C.B. (1983) Edge and Line Detection on Multidimensional Noisy Imagery Data. IEEE Transaction on Geoscience and Remote Sensing, GE-21(2), p. 163-174.

- [16] Cleynenbreugel, J.V., et al. (1990) Delineating Road Structures on Satellite Imagery by a GIS-guided Technique. Photogrammetric Engineering and Remote Sensing, vol.56, p. 893-893.

20

- [17] Wang, J.F., et Newkirk, R. (1988) Knowledge-Based System for Highway Network Extraction. IEEE Transaction on Geoscience and Remote Sensing, vol.26, n° 5, p. 525-531.

- 25 [18] Yee, B. (1987) An Expert System for Planimetric Feature Extraction. Processing of IGARSS 87, Ursi, Ann Arbor, Michigan, p. 321-325.
-

- [19] Farah, Noureddine. (1998) Extraction et évaluation du réseau routier urbain à partir des images satellitaires : développement d'algorithmes. Mémoire de maîtrise, Université de Sherbrooke, Sherbrooke, 112 p.
- 5 [20] Jedynek, Bruno. (1995) Modèles stochastiques et méthodes déterministes pour extraire les routes des images de la Terre vues du ciel. Thèse de doctorat. Université Paris Sud, UFR de mathématiques. 185 p.
- 10 [21] Copeland, A.C., Ravichandran, G. et Trivedi, M. M. (1994) Localized Radon Transform-Based Detection of Linear Features in Noisy Images. Proc. IEEE Conf. On Computer Vision and Pattern Recognition, Seattle, WA, Juin 1994, p. 664 – 667.
- 15 [22] Duda, R. O. et Hart, P. E., (1972) Use of the Hough Transformation to Detect Lines and Curves in Pictures. Comm. ACM, 15(1), p. 11 – 15.
- 20 [23] Murphy, L. M., (1986) Linear Feature Detection and Enhancement in Noisy Images Via the Radon Transformation. Pattern Recognition Letters, 4(4), p. 279 – 284.
- 25 [24] Rey, M. T. et al., (1990) Application of Radon Transform Techniques to Wake Detection in Seasat-A SAR Images. IEEE Trans. Geoscience and Remote Sensing, 28(4), p. 553 – 560.
- 30 [25] Karnieli, A. et al., (1996) Automatic Extraction and Evaluation of Geological Linear Features from Digital Remote Sensing Data Using a Hough Transform. Photogrammetric Engineering & Remote Sensing, Vol. 62, No. 5, May 1996, pp. 525 – 531.
-

5 [26] Toft, P. (1996) The Radon Transform, Theory and  
Implementation. These de doctorate, Department of Mathematical  
Modelling, Section for Digital Signal Processing, Technical University  
of Denmark, 308 p.

10 [27] Wang, J.F. (1993) LINDA - A System for Automated Linear Feature  
Detection and Analysis. Canadian Journal of Remote Sensing, vol.19,  
n° 1, p. 9-21

15 Although the present invention has been described  
hereinabove by way of preferred embodiments thereof, it can be modified,  
without departing from the spirit and nature of the subject invention as  
defined in the appended claims.

---

**WHAT IS CLAIMED IS:**

1. A method for the automatic extraction of linear features from digital imagery substantially as disclosed herein.

5

2. An apparatus for the automatic extraction of linear features from digital imagery substantially as disclosed herein.

---

FIGURE 1a

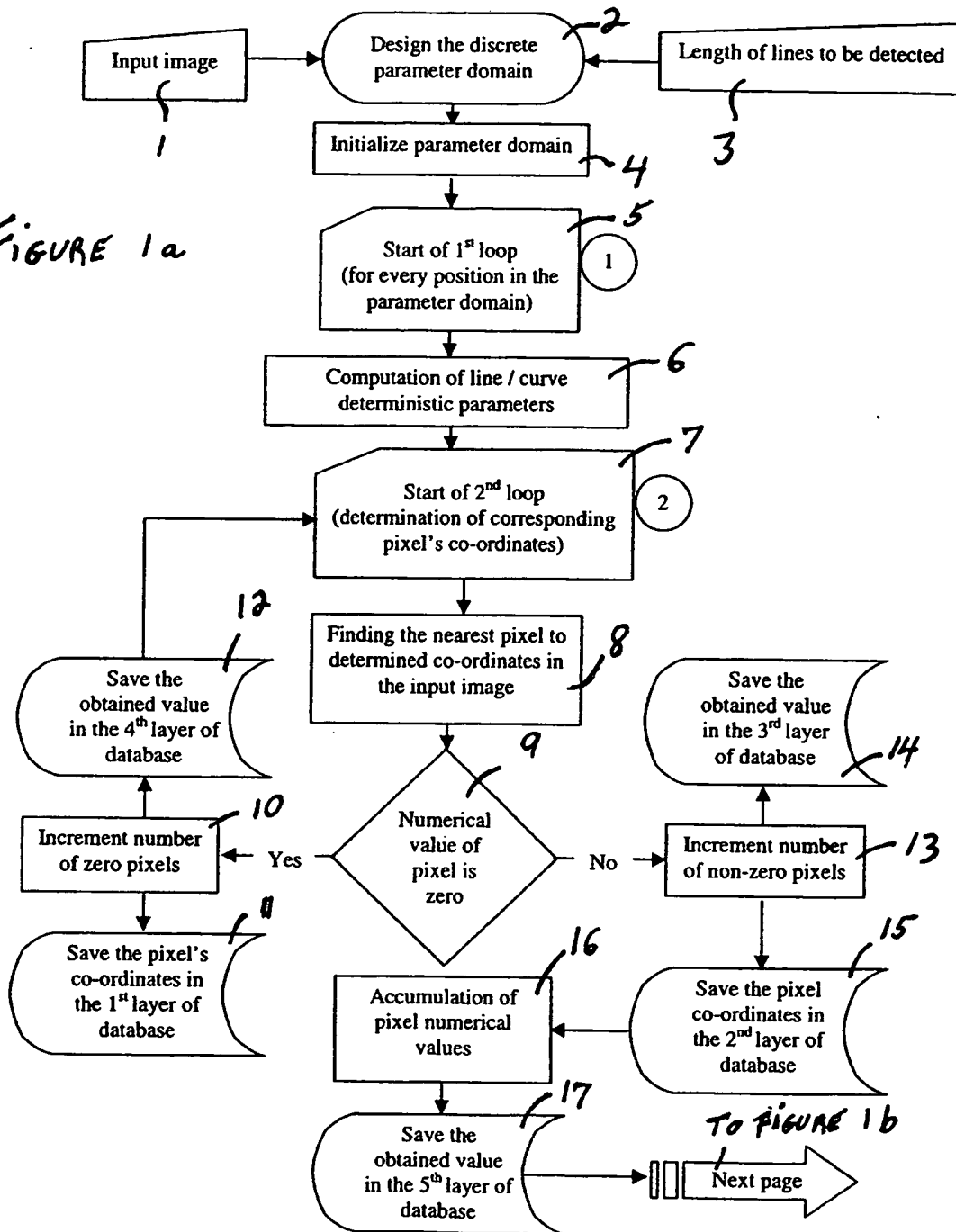
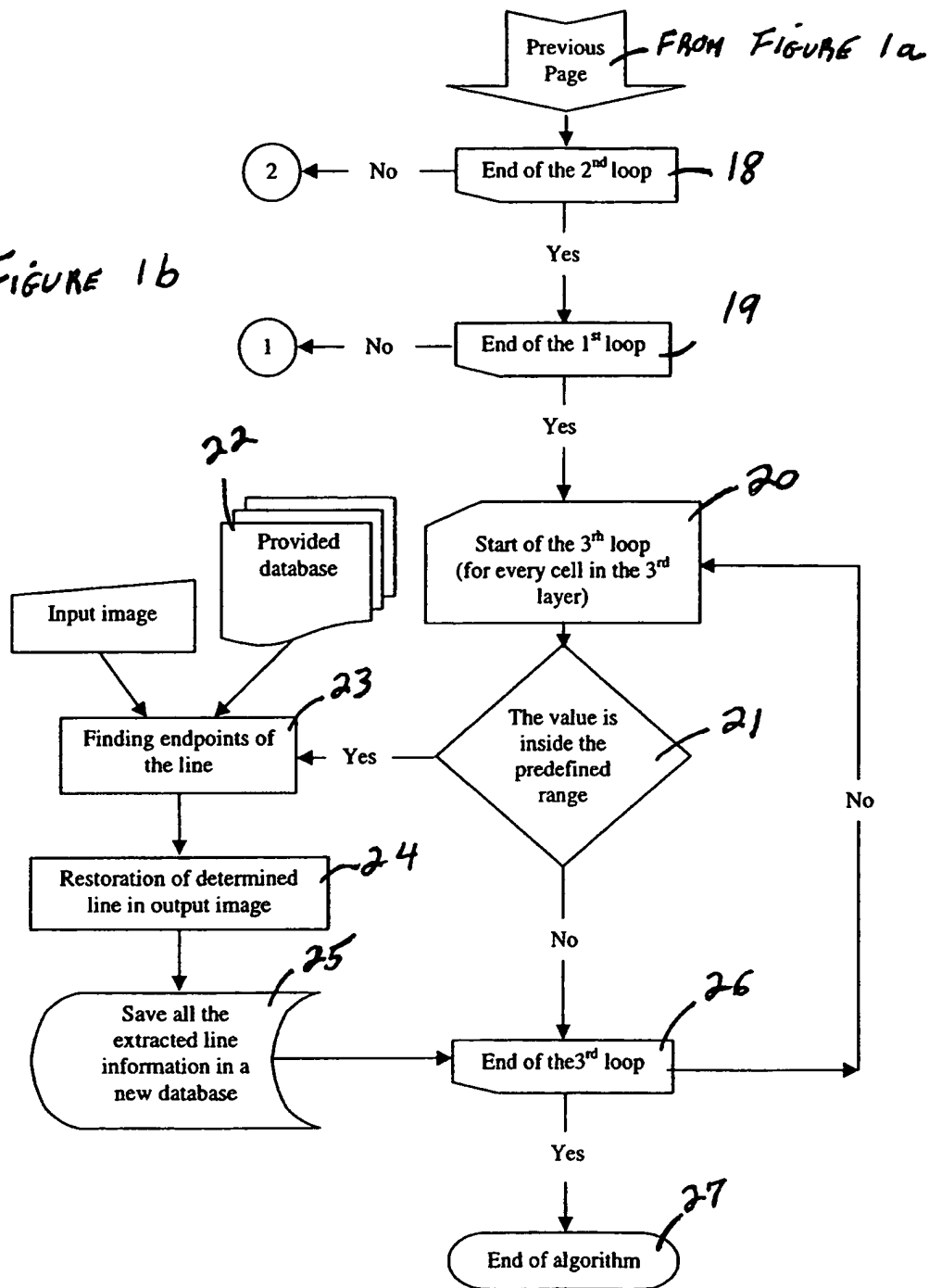


FIGURE 1b





**Flowchart legend**

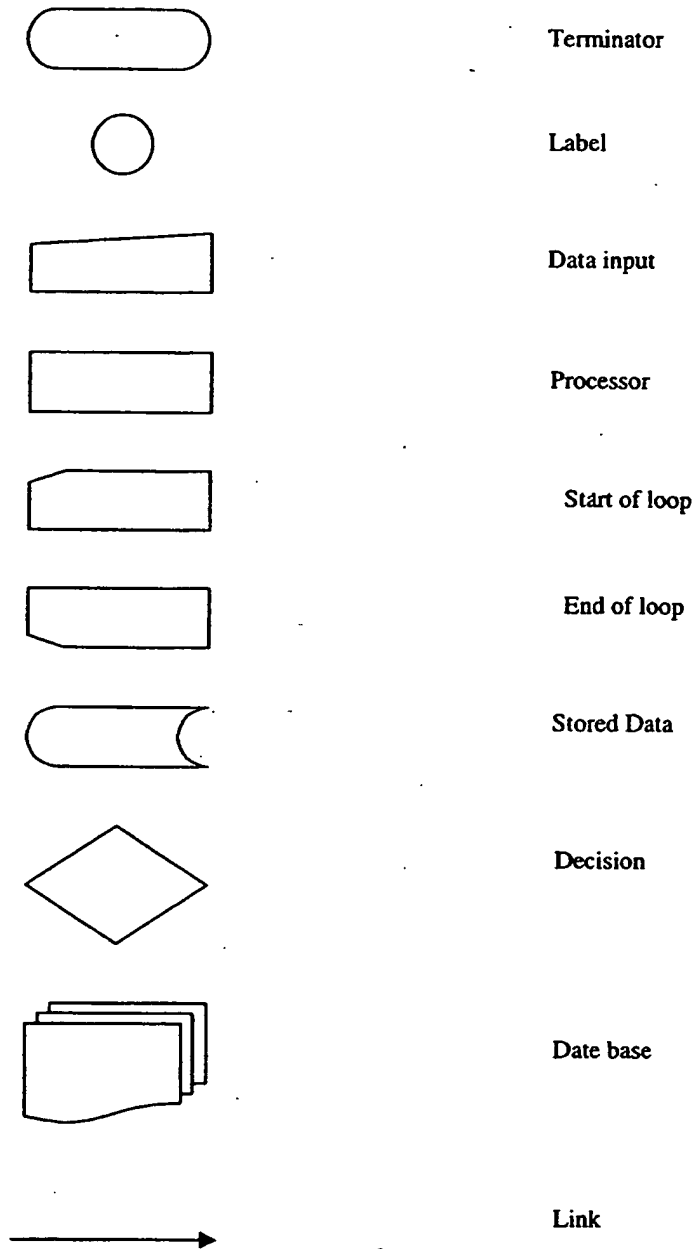


FIGURE 1c

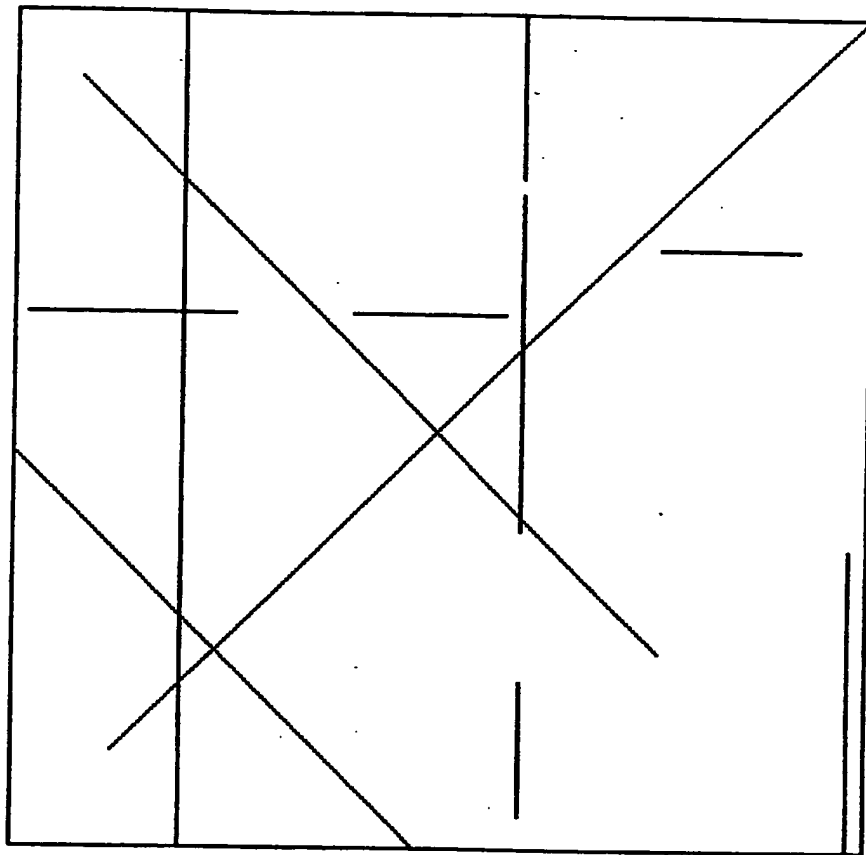


FIGURE 2

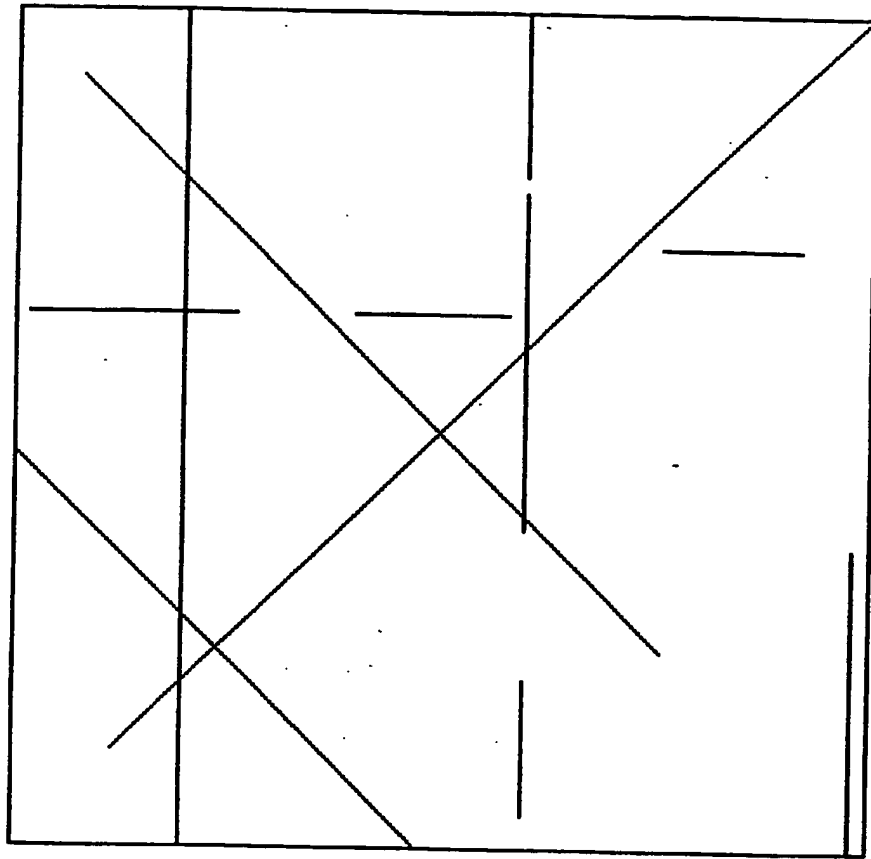


FIGURE 3

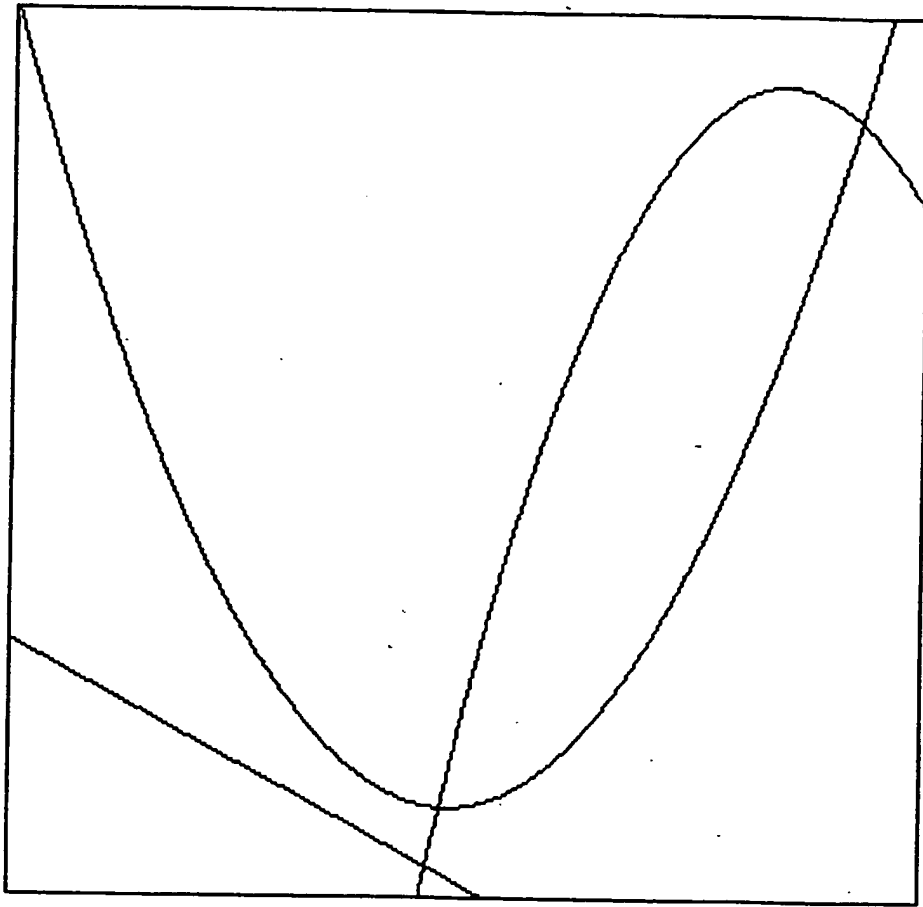


FIGURE 4

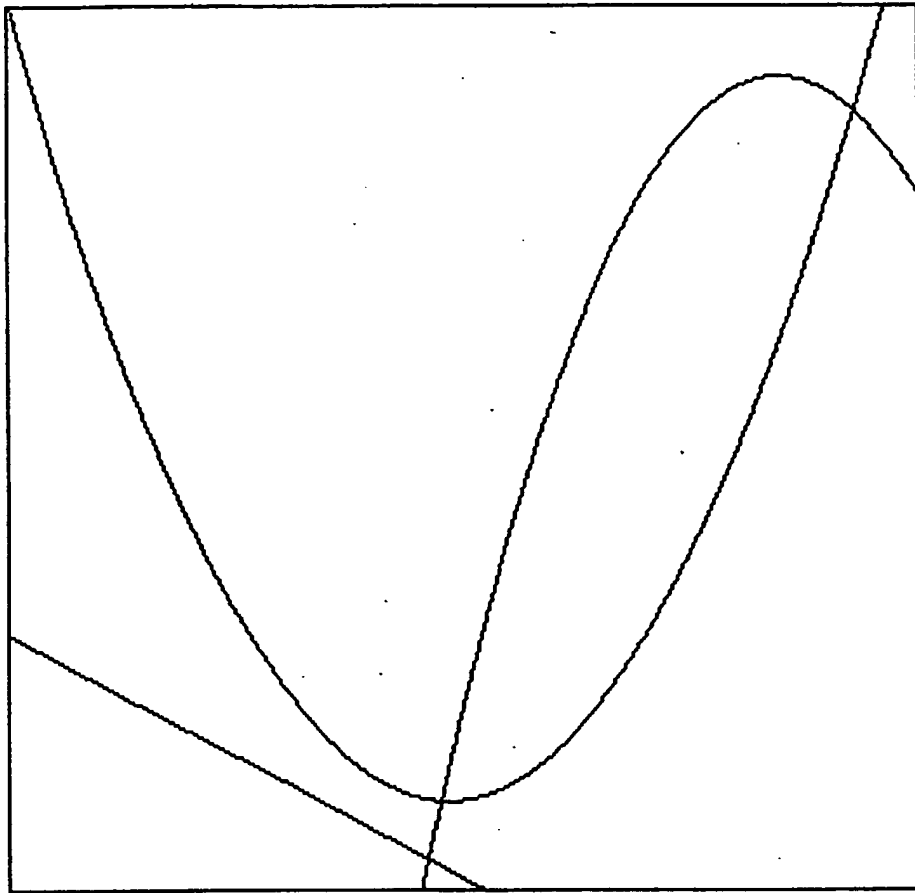
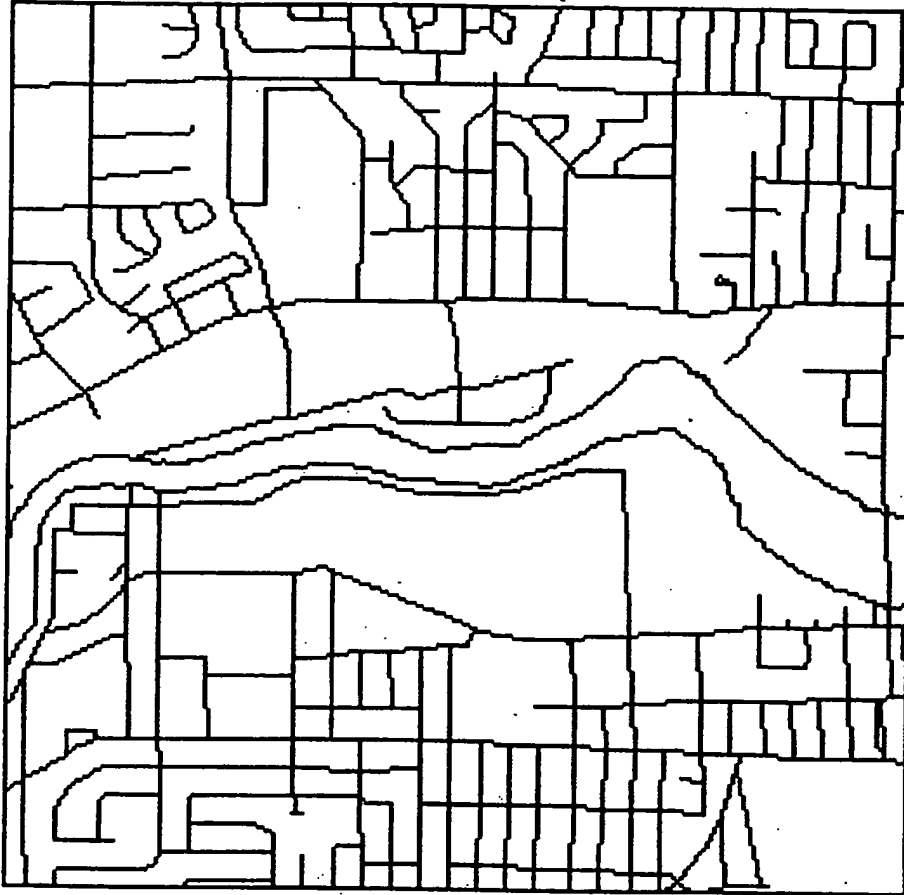


FIGURE 5



Portion of the digitized road map of the city of Sherbrooke

FIGURE 6

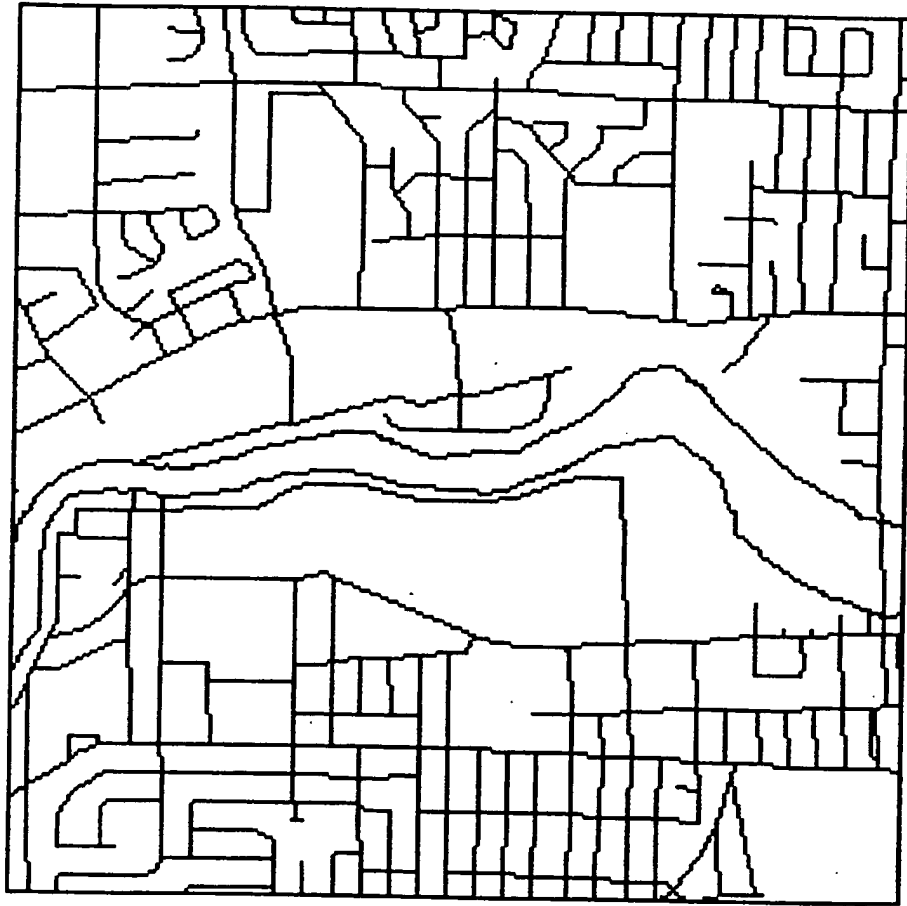


FIGURE 7

**This Page is Inserted by IFW Indexing and Scanning  
Operations and is not part of the Official Record**

**BEST AVAILABLE IMAGES**

Defective images within this document are accurate representations of the original documents submitted by the applicant.

Defects in the images include but are not limited to the items checked:

- ☐ BLACK BORDERS
- ☐ IMAGE CUT OFF AT TOP, BOTTOM OR SIDES
- ☐ FADED TEXT OR DRAWING
- ☐ BLURRED OR ILLEGIBLE TEXT OR DRAWING
- ☐ SKEWED/SLANTED IMAGES
- ☐ COLOR OR BLACK AND WHITE PHOTOGRAPHS
- ☐ GRAY SCALE DOCUMENTS
- ☐ LINES OR MARKS ON ORIGINAL DOCUMENT
- ☒ REFERENCE(S) OR EXHIBIT(S) SUBMITTED ARE POOR QUALITY
- ☐ OTHER: \_\_\_\_\_

**IMAGES ARE BEST AVAILABLE COPY.**

**As rescanning these documents will not correct the image problems checked, please do not report these problems to the IFW Image Problem Mailbox.**